Articles

Singular Efficacy of Trimethylamine *N*-Oxide to Counter Protein Destabilization in Ice

Giovanni B. Strambini* and Margherita Gonnelli

Consiglio Nazionale delle Ricerche, Istituto di Biofisica, 56124 Pisa, Italy

Received December 19, 2007; Revised Manuscript Received January 30, 2008

ABSTRACT: This study reports the first quantitative estimate of the thermodynamic stability ($\Delta G°$) of a protein in low-temperature partly frozen aqueous solutions in the presence of the protective osmolytes trimethylamine *N*-oxide (TMAO), glycine betaine, and sarcosine. The method, based on guanidinium chloride denaturation of the azurin mutant C112S from *Pseudomonas aeruginosa*, distinguishes between the deleterious effects of subfreezing temperatures from those due specifically to the formation of a solid ice phase. The results point out that in the liquid state molar concentrations of these osmolytes stabilize significantly the native fold and that their effect is maintained on cooling to −15 °C. At this temperature, freezing of the solution in the absence of any additive causes a progressive destabilization of the protein, $\Delta G°$ decreasing up to 3–4 kcal/mol as the fraction of liquid water in equilibrium with ice (V_L) is reduced to less than 1%. The ability of the three osmolytes to prevent the decrease in protein stability at small V_L varies significantly among them, ranging from the complete inertness of sarcosine to full protection by TMAO. The singular effectiveness of TMAO among the osmolytes tested until now is maintained high even at concentrations as low as 0.1 M when the additive stabilization of the protein in the liquid state is negligible. In all cases the reduction in $\Delta G°$ caused by the solidification of water correlates with the decrease in *m*-value entailing that protein−ice interactions generally conduct to partial unfolding of the native state. It is proposed that the remarkable effectiveness of TMAO to counter the ice perturbation is owed to binding of the osmolyte to ice, thereby inhibiting protein adsorption to the solid phase.

Low, subfreezing temperatures have dramatic consequences for many living organisms. Among the causes of freeze injury and death is the cold lability of protein molecules (*1*). Both prokaryotic and eukaryotic cells adopt a common strategy in protecting their proteins by producing or importing low molecular weight organic substances called osmolytes (*2–4*). Osmolytes can be grouped into three major classes: polyols, amino acids, and methylammonium compounds. Often they are further classified as compatible or counteracting on the basis of their effect on the functional activity of proteins. Compatible osmolytes increase protein stability against denaturation with little or no effect on their function (*2, 5–7*), whereas counteracting osmolytes have in addition the ability to offset the deleterious effects of urea, hydrostatic pressure, and low temperature on the catalytic activity (*2, 4, 8–13*).

Prominent among counteracting osmolytes are the methylamines glycine betaine (betaine), sarcosine, and trimethylamine *N*-oxide (TMAO).[1] Numerous studies, in particular with TMAO, have demonstrated their efficacy toward increasing protein stability (raise $\Delta G°$ and T_m) (*10, 14–17*), force folding of unstructured proteins (*6, 12, 13, 18, 19*), and correct temperature-sensitive misfolding and aggregation (chemical chaperone activity) (*20*). Several arctic fishes living at subzero temperatures have high levels of TMAO for reasons that are not fully understood but that might have to do with prevention of protein cold denaturation (*21*). The effectiveness of these compounds has been correlated to the degree of preferential exclusion of the cosolvent from the protein surface (*10, 14*), which at the molecular level has been attributed predominantly to the repulsive interaction between osmolyte and peptide backbone (*22–24*). Despite the numerous studies describing the effects of these methylamines in liquid solutions, to date practically no data are available on their influence on the stability of proteins in partly frozen solutions.

In vitro, freeze–thawing of protein solutions may result in irreversible protein aggregation and severe loss of catalytic activity of enzymes, reasons for which many proteins cannot be stored in ice or lyophilized from it without partial inhibition of their function. Elucidation of protection mechanisms against freeze damage would shed light on the survival strategies of psychrophilic organisms but would also have practical applications in developing formulations and protocols aimed to stabilize pharmacoproteins during indus-

* Corresponding author. Tel: +39 050 315 3046. Fax: +39 050 315 2760. E-mail: strambini@pi.ibf.cnr.it.

[1] Abbreviations: Caz, mutant C112S of azurin from *Pseudomonas aeruginosa*; Gdn, guanidinium chloride; TMAO, trimethylamine *N*-oxide.

10.1021/bi702473g CCC: $40.75
Published on Web 02/23/2008

trial freeze-drying processes. Until recently, however, determination of protein stability in ice and, consequently, of the osmolyte ability in preserving the native fold has been withheld by the intrinsic complexity of frozen solutions, challenging quantitative evaluation of chemical eqiulibria in this medium by ordinary spectroscopic techniques. Indeed, frozen samples are highly scattering and heterogeneous with a spatially uneven concentration of solutes. Optical signals exhibit large site-to-site variation in intensity and are invariably associated to a conspicuous and unsteady background. The concentration of some solutes in the liquid phase can be uncertain as below their eutectic temperature they may crystallize out or remain in an undercooled state or even separate out into distinct amorphous phases (*25*). Depending on the cosolutes, the liquidus viscosity can increase to such a point that protein unfolding eqiulibria are severely slowed and may be difficult to separate kinetic from thermodynamic effects. Time and again the reversibility of unfolding eqiulibria is compromised by intermolecular protein–protein interactions elicited by the large, over hundred-fold freeze concentration factor.

Recently, an experimental approach was developed in this laboratory, based on laser-excited CCD-detected Trp fluorescence, capable of determining protein unfolding eqiulibria in ice. A suitable model protein was found, the mutant C112S of azurin from *Pseudomonas aeruginosa* (Caz), that in the presence of guanidinium chloride denatures rapidly and reversibly both in liquid and in frozen solutions, thus providing an assessment of its thermodynamic stability ($\Delta G°$) in ice (*26*). It was shown for the first time that the solidification of water poses a significant stress on the native fold, $\Delta G°$ decreasing up to 30–40% as the liquid water pool in equilibrium with ice shrinks to below 1%. Unexpectedly, the addition of popular sugars (sucrose and trehalose) and polyols (sorbitol and glycerol), commonly employed to preserve the activity of pharmacoproteins during freeze-drying, did not attenuate the ice perturbation, suggesting that cryoprotection by polyhydric compounds is probably of a kinetic rather than thermodynamic nature.

In this work we apply the methodology to evaluate the effectiveness of the counteracting osmolytes TMAO, betaine, and sarcosine on the stability of C112S azurin in both liquid and partly frozen solutions at −15 °C. The results emphasize that although protein stabilization by the three methylamines is comparable in low-temperature liquid solutions, their effectiveness varies dramatically in ice.

MATERIALS AND METHODS

All chemicals were of the highest purity grade available from commercial sources and unless specified to the contrary were used without further purification. Tris(hydroxymethyl)-aminomethane (Tris) and NaCl Suprapur were from Merck (Darmstadt, Germany). Guanidinium chloride (Gdn), TMAO, glycine betaine, and sarcosine were from Sigma-Aldrich (Deisenhofen, Germany). On visual inspection TMAO showed white colorless crystals practically free of the fishy smell given by TMA^+. Prior to use, concentrated sarcosine solutions were treated with activated charcoal (Aldrich) and filtered through a 0.22 mm sterile filter (Millipore Millex GP). Its molar concentration was determined by refractive index. The concentration of Gdn was determined by refractive index (*27*) and confirmed by density measurements (*28*). Water, doubly distilled over quartz, was purified by a Milli-Q Plus system (Millipore Corp., Bedford, MA).

Protein Expression and Purification. The preparation of C112S azurin was done following a procedure analogous to that described by Karlsson et al. (*29*) for the wild-type protein except for the omission of any $CuSO_4$ addition in both growth and purification medium (*30*). The plasmid carrying the wild-type sequence was a generous gift of Prof. A. Desideri (Università di Roma, "Tor Vergata"). The C112A mutant was constructed using the QuikChange kit (Stratagene, La Jolla, CA) and confirmed by sequencing.

Sample Preparation for Denaturation Experiments in Liquid and Frozen Solutions. It must be stressed that with frozen samples fine control of the concentration of *each* solute in the denaturation mixture is crucial for the reproducibility of unfolding eqiulibria and the precision of the derived thermodynamic parameters. To this end we adopted rigorous gravimetric control of sample composition and prepared all samples for denaturation in ice by diluting with water the original solute mixtures used for denaturation in liquid solutions, a procedure that assures exactly the same composition of solutes in the liquidus at all V_L examined. For each methylamine, equilibrium denaturation profiles in *liquid* solutions (at 20 and −15 °C) were obtained by examining a series of about 25 azurin samples, appositely prepared to contain a constant amount (1.2 M) of a methylamine (additive), a variable concentration of denaturant (Gdn), and a balancing amount of NaCl (reference salt) as required to maintain the freezing temperature (T_f) of the solution close to −15 °C, the temperature of denaturation experiments in ice. The samples (10 μM in protein, 150 μL volume) were prepared by adding 20 μL of protein stock (75 μM, in 0.1 mM Tris, pH 7.5) to 130 μL of appositely prepared solvent mixtures, here referred to as mother mixtures (mxs), containing Gdn, NaCl, and additive, spanning a range of Gdn concentrations sufficient to fully denature the protein. mxs were prepared gravimetrically from two parent stock solutions (stocks B), equimolar in additive, one containing Gdn and the other NaCl, the concentration of either salt adjusted to exhibit a T_f close to −15 °C, when diluted with the protein aliquot (130 + 20 μL). Stocks B, in turn, were prepared gravimetrically by adding to 50 mL volumetric flasks the required amount of methylamine plus Gdn (8.1 M) or NaCl (5.0 M). Their pH was adjusted to between 7.2 and 7.5 with 30 mM Tris. Each series is labeled according to the additive: NaCl reference (no additive), TMAO, betaine, and sarcosine.

Frozen samples are characterized by a solid phase of pure water (ice) in equilibrium with a liquid phase (liquidus) comprising liquid water and practically all of the solutes (protein, salts, and additives) at relatively high concentration, $[\text{solutes}]_{\text{liquidus}}$. The samples for denaturation experiments in *ice* were prepared in the same fashion as above, but subsequent to diluting the mxs from about 2- to 200-fold with pure water. Because the starting liquid samples from which they are prepared have a $T_f \approx -15$ °C, at this temperature, any water added to these solutions will freeze out, leaving a liquidus of exactly the same composition of the original stock. For any given dilution, the magnitude of V_L of the corresponding frozen sample is simply given by $V_L = [\text{solutes}]_{\text{liquid}}/[\text{solutes}]_{\text{liquidus}}$ (from the equality $1[\text{solutes}]_{\text{liquid}} = V_L[\text{solutes}]_{\text{liquidus}}$ and $V_L = 1$ in the liquid state).

In these experiments V_L ranged from 0.53% to 53%, which corresponds to total solute concentrations in the starting liquid state, at 20 °C, ranging from about 0.020 to about 2.0 M.

Frozen samples were prepared by placing liquid samples (150 μL) in capped spectrosil quartz tubing, 4 mm i.d., and freezing them in a cold bath (−20 °C). Subsequently, ice was melted leaving a small seed from which new ice was formed at the bath temperature, set at −15 °C, the temperature of the experiment. This procedure improved signal reproducibility, when compared to freezing by sudden cooling the solution to very low temperatures, presumably because of a more even spatial distribution of solutes in frozen samples. No phase separation due solute crystallization in ice was observed in any of the samples examined in this study. This is consistent with eutectic temperatures for NaCl and Gdn lower than −15 °C (−21 and −24 °C, respectively) and the observation that the methylamines do not crystallize out under these conditions.

For each methylamine and salt reference at least two independent series, each of 25 protein samples, were prepared for every value of V_L (100%, 53%, 2.7%, and 0.53%), and the fluorescence spectrum of frozen samples was measured again after melting and refreezing the samples. In all, over 1200 protein samples have been examined and over 2400 fluorescence spectra have been measured. The results reported here represent the average values from these measurements.

Determination of Freezing Temperatures. In the preparation of stocks B (having a T_f close to −15 °C) the concentration of NaCl and Gdn needed to be adjusted for each methylamine by means of freezing point determinations. For the determination of freezing temperatures 1 mL samples were placed in a long round quartz cell (4 mm i.d.), sealed off from the atmosphere, and slowly frozen in a cold ethanol–water bath (−20 °C) to avoid cracking of the cell. After 0.5 h equilibration the bath temperature was raised by consecutive 0.05 °C steps intercalated by 10 min equilibration time after each temperature change. Before ice was completely melted the solution was gently stirred (by means of a temperature-equilibrated thin plastic rod) to eliminate any temperature and concentration gradient through the sample. The freezing temperature, measured with a precision (0.001 °C) thermometer (model 1502; Hart Scientific, American Fork, UT), was the temperature of the bath at which no further ice could be detected. The reproducibility of T_f measurements was generally better than 0.1 °C.

Analysis of Denaturation Profiles in Frozen Samples. The analysis of denaturation profiles in ice requires knowledge of the denaturant concentration in the liquidus, $[Gdn]_{liquidus}$. This is given by the $[Gdn]_{liquid}$ times the freeze concentration factor. Usually the latter is derived for each solute by determining the liquidus curve for every change of sample composition (Gdn concentration). However, because it requires a large number of freezing point determinations, this procedure is lengthy and time-consuming, even with modern freezing point determination methods based on differential scanning calorimetry (*31*). In this and previous studies we adopted a less rigorous but simpler approach. It takes advantage of the fact that when the amount of ice is small, i.e., in *predominantly liquid* samples (V_L > 96%), the $\Delta G°$ and *m*-value of frozen solutions are expected to be the same as those of *liquid* solutions. We then determined the effects of this approximation by comparing the thermodynamic parameters obtained from isothermal denaturation curves with predominantly liquid (V_L > 96%) and liquid samples, both plotted against the [Gdn] in the liquid state. In general, the procedure yields a few percent larger estimate of $\Delta G°$ and *m*-value from the denaturation profiles in ice. Consequently, all $\Delta G°$ and *m*-values obtained with frozen samples have been multiplied by the correcting factors f_c reported in Table 1 and determined as follows. Liquid samples were prepared to have a freezing temperature a little higher (typically 0.1–0.2 deg) than −15 °C and were first analyzed in the liquid state at −15 °C. Subsequently, they were frozen in liquid nitrogen and then let to equilibrate at −15 °C for 2 h before a new denaturation curve was determined after adequate stirring. Because the freezing temperature is slightly higher than −15 °C, a small amount of water remained frozen and a tiny ice ring floated on top of each sample. The factor f_c represents the ratios $\Delta G°$(liquid)/$\Delta G°$(liquidus) and *m*(liquid)/*m*(liquidus) obtained from the analysis of these denaturation profiles using the [Gdn] in liquid solutions at 20 °C. This procedure is rapid, and the assumption that the protein stability is not affected by a small amount of ice is quite reasonable as for V_L > 50% no difference in $\Delta G°$ and *m*-value could be found between liquid and frozen samples (*26*).

Table 1: Sample Composition, Isosbestic Wavelength (λ_{iso}), and Liquid to Ice Correction Factor (f_c)

sample	[NaCl] (M)	[additive] (M)	λ_{iso} (20 °C) (nm)	λ_{iso} (−15 °C) (nm)	f_c ($\Delta G°$)	f_c (*m*)
TMAO	2.52	1.16	344.5	334.4	0.94	0.91
TMAO	3.00	0.60	344.5	334.7	0.93	0.90
TMAO	3.50	0.10	345.0	337.5	0.97	0.94
betaine	2.50	1.20	341.5	334.2	0.95	0.90
sarcosine	3.00	1.20	349.2	340.5	0.96	0.94

Fluorescence Measurements. Prior to fluorescence measurements liquid and frozen samples were equilibrated for at least 2 h at the bath temperature and then rapidly transferred to the sample holder of the fluorometer, set at the same temperature. Kinetic runs following temperature jumps showed that a 10−15 min equilibration time was sufficient to give a constant degree of denaturation both in ice and in liquid solution, which remained invariant over a period of 1 week.

Fluorescence spectra were measured on a homemade apparatus that implements pulsed UV laser excitation and emission detection by means of a CCD camera. The main advantage of laser over traditional lamp−monochromator sources is a considerable reduction of the spurious background signal, while the merit of CCD detection over the traditional scanning monochromator−photomultiplier assembly is simultaneous acquisition of the entire spectrum. The latter is crucial for avoiding spectral distortions caused by instability of excitation intensity, changes in excitation/collection efficiency of the optical system, and transmittance of the medium during spectral acquisition. Pulsed excitation (λ_{ex} = 288 nm), horizontally polarized with respect to the optical plane, was provided by a frequency-doubled Nd/Yag-pumped dye laser (Quanta Systems, Milan, Italy) with pulse duration of 5 ns, pulse frequency up to 10 Hz, and energy per pulse varying from 10 to 1000 μJ. The emission collected at 90° from the excitation direction was passed through a 290 nm long-pass filter (WG290; Lot-Oriel, Milan, Italy)

and dispersed by a 0.3 m focal length triple grating imaging spectrograph (SpectraPro-2300i; Acton Research Corp., Acton, MA) set to a band-pass of 2.0 nm. The emission intensity in the spectral range 295–435 nm was monitored by a back-illuminated 1340 × 400 pixel CCD camera (Princeton Instruments Spec-10:400B (XTE); Roper Scientific Inc., Trenton, NJ) cooled to −60 °C. Fluorescence intensity variations among frozen samples were reduced by rotating the sample (3 Hz) during spectral acquisition and by averaging 8–10 pulses during 1.5 s acquisition time. To avoid vapor condensation on optical components, the whole apparatus was maintained under nitrogen atmosphere.

Data Analysis. The fraction of native azurin, f_N, in the denaturation equilibrium was determined by two alternative approaches by assuming a two-state equilibrium. One is based on the fluorescence intensity ratio $R = F_{308}/F_{357}$ according to the relationship (*26*)

$$f_N = ({}^D f_{308} - R\,{}^D f_{357})/(R\Delta_{357} - \Delta_{308}) \quad (1)$$

where $\Delta_\lambda = {}^N f_\lambda - {}^D f_\lambda$. ${}^N f_\lambda = {}^N F_\lambda/F_{\lambda iso}$ and ${}^D f_\lambda = {}^D F_\lambda/F_{\lambda iso}$ are the fluorescence intensities at wavelength λ of native and fully denatured azurin, respectively, normalized by the fluorescence intensity at the isosbestic point, $F_{\lambda iso}$.

The other method is based on the shift of the center of spectral mass of the fluorescence spectrum, $v_g = \sum v_i F_i/\sum F_i$, F_i the fluorescence intensity at $v_i = 1/\lambda_i$, according to the relationship (*32*)

$$f_N = [1 + (v - v^D)/(v^N - v)\varphi]^{-1} \quad (2)$$

where v^N and v^D are the center of spectral mass of native and denatured azurin, respectively, and φ is the ratio of their fluorescence quantum yields, φ^D/φ^N. The parameter φ^D/φ^N is given by the ratio $\sum F_i^D/\sum F_i^N$ as obtained from the fluorescence spectrum of D and N, each normalized at λ_{iso}.

It should be noted that the above expressions for f_N take into account all variations of molar absorptivity and fluorescence yield between N and D states of the protein and, moreover, they are totally independent of excitation intensity, extent of light scattering in frozen samples, and protein concentration within the exciting beam. Note also that because the fluorescence yield varies substantially with temperature and the additive employed, in particular for D, the parameters of eqs 1 and 2 and the isosbestic point were determined for each additive both at +20 and at −15 °C, the two temperatures examined here. The isosbestic points are collected in Table 1.

The agreement in the estimate of f_N by the two methods was excellent throughout, even if the reproducibility was slightly superior with the use of the center of mass.

The thermodynamic parameters $\Delta G°$, *m*-value, and $D_{1/2}$ (the midpoint denaturant concentration) describing the unfolding transition were derived from nonlinear least-squares fitting of f_N data to the expression $f_N = 1/\{1 + \exp[-(\Delta G° - m[\mathrm{Gdn}])/RT]\}$ (*33–35*). The data were fitted using the program Origin 7 (Originlab Corp.).

It should be pointed out that the estimate of $\Delta G°$ is subject to the validity of the linear extrapolation method, LEM, when Gdn is the denaturant. Concern has sometimes been raised that with some proteins, particularly if sensitive to the ionic strength of the medium, $\Delta G°$ estimated by LEM using Gdn may differ from that obtained using urea as denaturant and that in general the latter is in better agreement with calorimetric studies. The reason may lie on a different reference state, dilute buffer for urea vs molar salt concentration for Gdn, respectively, but also on a nonlinearity in the Gdn free energy plot. To address this concern, we have repeated the denaturation of azurin in dilute buffer employing urea as denaturant. The results demonstrate that the estimate of azurin stability is, within experimental error, exactly the same between urea and Gdn. For studies of protein stability in ice the use of Gdn/NaCl salt mixture is an obligatory choice, as it permits to maintain constant conditions of freezing temperature, pH, and ionic strength across the range of denaturant concentrations required to unfold the protein. Urea, on the other hand, is unsuitable for denaturation experiments in ice because the much larger concentration required compared to Gdn would lower the freezing temperature of the samples to far below its eutectic temperature (−13 °C).

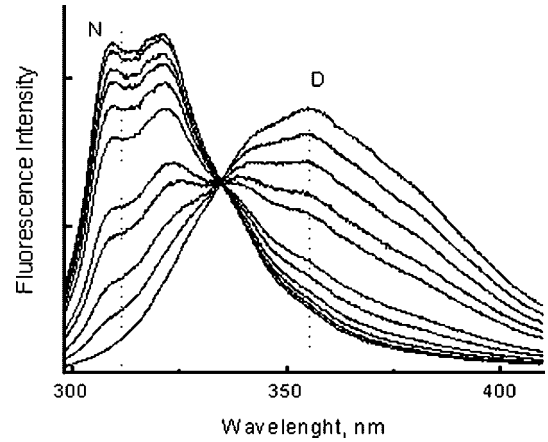

FIGURE 1: Changes in the fluorescence spectrum and intensity that characterize the denaturation of C112S azurin (10 μM) in frozen samples at –15 °C. The spectra refer to samples (V_L = 2.7%) containing a 31 mM TMAO and 68–70 mM Gdn/NaCl salt mixture ranging from 0% to 100% in Gdn content (all concentrations are referred to liquid solutions at 20 °C). N and D refer to the spectrum of native and fully denatured protein. Vertical dashed lines indicate the wavelengths used to calculate the fluorescence intensity ratio *R*. The excitation wavelength is 288 nm. All spectra are corrected for the instrumental response.

RESULTS

Figure 1 shows a typical example of the changes in the fluorescence spectrum and intensity (λ_{ex} = 288 nm) that characterize Caz denaturation. The spectra refer to samples (V_L = 2.7%) in the frozen state at −15 °C containing a 31 mM TMAO and 68–70 mM Gdn/NaCl salt mixture, ranging from 0% to 100% in Gdn content (all concentrations are referred to liquid solutions at 20 °C). We note the large spectral difference between N and D states, a feature that permits to determine with great precision the extent of unfolding and a clearly identified isosbestic point characteristic of two-state reactions. Throughout, N and D spectra are practically identical between liquid and frozen state, the only difference being a somewhat larger background contribution with frozen samples. As pointed out before (*26*), background subtraction was not found to be necessary as it had negligible effects on the estimate of f_N.

Caz denaturation in liquid and frozen solutions was found to be completely reversible irrespective of the methylamine

employed. In ice, reversibility was indicated by complete recovery of the native fluorescence upon thawing fully denatured samples as well as by promptly reversible shifts on the equilibrium following up or down temperature jumps. The lack of hysteresis in the unfolding equilibrium, even after several consecutive cooling−warming cycles, is consistent with a highly reversible process that excludes the formation of protein aggregates (a condition not met by the wild-type protein).

The kinetics of azurin unfolding in ice, at −15 °C, was assessed by the decrease of f_N following a rapid drop in freezing temperature from −10 to −15 °C. In frozen samples, the denaturant concentration in the liquidus varies sharply with freezing temperature, and when the system is poised near the transition, a temperature drop of 5 °C is sufficient to shift the equilibrium from predominantly native to predominantly denatured. Frozen samples of suitable Gdn concentration were first equilibrated in a bath at −10 °C and then transferred to the fluorometer sample holder held at −15 °C, where it took about 20 s to equilibrate to the colder temperature. Because of the cooling dead time the method is limited to equilibrium half-lives greater than 0.5 min. For frozen samples of $V_L = 2.7\%$ the exponential decrease of f_N in time yielded half-lives that ranged among methylamines between 2 and 3.5 min, values that were found to be largely independent of V_L.

Spatial Uniformity of f_N in Ice. Ice is a spatially nonuniform medium in which the distribution of solutes can vary from one site to another, depending on the ice growth rate and the direction of the thermal gradient during freezing. Tests devised to check the spatial uniformity of the degree of azurin denaturation consisted of measuring the fluorescence spectrum in different positions of the sample after reducing the excitation beam diameter from 2.5 (normal) to 0.5 mm to enhance spatial resolution. The results obtained with frozen samples with f_N values close to 0.5, for maximum sensitivity, indicated right through that, despite an up to 2.5-fold variation of the fluorescence intensity across the sample, presumably reflecting distinct excitation/fluorescence collection efficiencies or spatially nonuniform protein concentration, no significant differences could be detected in the degree of denaturation. Thus, it appears that at this spatial resolution both the liquidus composition and the stability of azurin in ice are uniform throughout.

Effect of Methylamines on the Stability of Caz in Liquid Solutions at 20 and −15 °C. Figure 2 compares the effect of 1.2 M osmolyte on the equilibrium unfolding curve at 20 °C. The shift of the profile to higher denaturant concentrations confirms that TMAO, betaine, and sarcosine all stabilize the native fold of azurin. The parameters $\Delta G°$ and *m*-value obtained by least-squares fitting a two-state model to the data are collected in Table 2. $D_{1/2}$ represents the ratio $\Delta G°/m$. For the NaCl reference the data are in good agreement with previous values reported by Sandberg et al. (*36*) and by our previous study (*26*). The increase in $\Delta G°$ is largest with betaine (+2.1 kcal/mol) and smallest with sarcosine (+1.0 kcal/mol). In the case of TMAO it is 1.57 kcal/mol, which when normalized to 1 M osmolyte concentration is similar to the 1–1.3 kcal/mol increase in $\Delta G°$ obtained from thermal denaturation studies of lysozyme, ribonuclease A, and apo-α-lactalbumin (*37*). The *m*-value, which is a measure of the denaturant effectiveness to unfold the protein, is practically

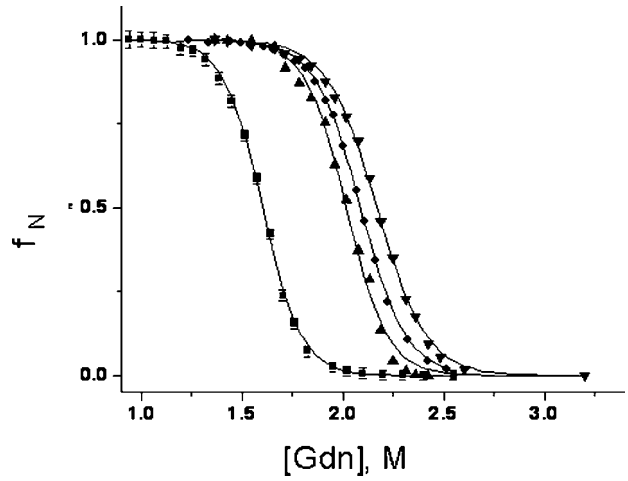

FIGURE 2: Equilibrium denaturation curves of C112S azurin (10 μM) at 20 °C for (■) salt reference, (●) TMAO, (▼) sarcosine, and (▲) and betaine. Error bars are shown only for salt reference.

identical between NaCl reference and betaine [$m = 5.83$ kcal/(mol·M)] but decreases to 5.2 and 4.7 kcal/(mol·M) for TMAO and sarcosine, respectively. The slightly lower denaturing efficacy of Gdn in the presence of TMAO and sarcosine suggests that osmolyte and denaturant do not act independently on the protein but presumably compete for some common interaction sites. In comparison to Gdn, TMAO did not alter the ability of urea to unfold barnase or the notch ankyrin domains (*15*) nor did sarcosine change urea denaturation of the notch receptor subfragment Nank 4–7 (*38*), the difference between denaturants presumably reflecting the weaker affinity of urea, relative to Gdn, for the protein interaction sites.

Lowering the temperature from 20 to −15 °C has little effect on $\Delta G°$ of salt reference, TMAO, and sarcosine as its variation is within the range of the experimental error (Table 2). For betaine the stabilizing effect shown at ambient temperature is reduced at −15 °C and becomes similar to that of TMAO. Overall, the results show that the three methylamines remain good protein stabilizers even at subfreezing temperatures, a weak temperature dependence of $\Delta(\Delta G°)$ being consistent with the predominantly enthalpic nature of protein stabilization by TMAO (*37*).

In the analysis of low-temperature data, we have used Gdn concentrations that refer to 20 °C, which do not take into account the increase in solute concentration caused by cooling. While concentrations not corrected for cooling have no influence on the estimate of $\Delta G°$, they will yield larger apparent *m*-values. This factor might largely account for the generalized increase in *m*-values observed on cooling (Table 2).

Effect of the Methylamines on the Stability of Azurin in Ice. The only difference between frozen samples of decreasing V_L is that a proportionally greater fraction of water will form ice. Should the protein free energy in the liquidus, of either N or D state, not be perturbed by the amount of ice, the unfolding equilibrium and $\Delta G°$ would not be affected by freezing and be independent of V_L. Denaturations of frozen samples were obtained at three selected V_L (53%, 2.7%, and 0.53%), corresponding to dilution of the concentrated liquid samples to final total solute concentrations of about 2 M, 100 mM, and 20 mM, respectively. Figure 3

Table 2: Thermodynamic Parameters Relative to the Effects of Methylamines on the Denaturation of Caz in Liquid and Frozen Solutions at Selected V_L[a]

T (°C)	V_L (%)	additive	$\Delta G°$ (kcal/mol)	$\Delta(\Delta G°)$ (kcal/mol)	m-value [kcal/(M·mol)]	$D_{1/2}$ (M)
20	100	reference	9.3 ± 0.15		5.83 ± 0.19	1.59
		TMAO	10.87 ± 0.14	+1.57	5.21 ± 0.07	2.09
		betaine	11.39 ± 0.18	+2.09	5.82 ± 0.09	1.85
		sarcosine	10.26 ± 0.21	+0.96	4.73 ± 0.09	2.17
−15	100	reference	9.05 ± 0.21		6.69 ± 0.16	1.35
		TMAO	10.79 ± 0.14	+1.74	5.64 ± 0.07	1.91
		betaine	10.80 ± 0.12	+1.75	6.07 ± 0.07	1.78
		sarcosine	10.34 ± 0.15	+1.29	5.47 ± 0.08	1.90
−15	53	reference	9.40 ± 0.20		6.81 ± 0.22	1.38
		TMAO	10.5 ± 0.36	+1.10	5.50 ± 0.15	1.91
		betaine	11.19 ± 0.12	+1.79	6.34 ± 0.07	1.76
		sarcosine	9.95 ± 0.19	+0.55	5.21 ± 0.10	1.91
−15	2.7	reference	7.01 ± 0.27		5.02 ± 0.11	1.40
		TMAO	11.0 ± 0.24	+4.19	5.77 ± 0.12	1.94
		betaine	10.75 ± 0.20	+3.74	6.00 ± 0.12	1.79
		sarcosine	7.25 ± 0.14	+0.24	4.05 ± 0.08	1.79
−15	0.53	reference	5.90 ± 0.25		4.10 ± 0.17	1.44
		TMAO	10.3 ± 0.34	+4.40	5.34 ± 0.18	1.93
		betaine	7.43 ± 0.15	+1.53	4.11 ± 0.09	1.81
		sarcosine	6.45 ± 0.22	+0.55	3.52 ± 0.12	1.83

[a] The indicated errors represent the fitting error.

shows the effect of decreasing V_L from 53% and 0.53% on the unfolding transitions of NaCl reference, TMAO, betaine, and sarcosine. We first observe that, with very fine control of temperature and sample composition, the reproducibility of f_N measurements in ice and, therefore, the precision of the thermodynamic parameters derived from these transitions are comparable between liquid and frozen samples (see standard deviations, Table 2). The denaturation profiles in wet ice, at $V_L = 53\%$, are not significantly different from those in liquid solution at the same temperature (Table 2), demonstrating in all cases that the presence of a solid ice phase per se has by and large no direct effect on the stability of the protein. However, shrinking of the liquid water pool from 53% and 0.53% conducts, in the case of NaCl reference, betaine, and sarcosine, to a progressively less steep unfolding transition with minor shifts in the transition midpoint, $D_{1/2}$. The outcome is a significant decrease of both m-value and $\Delta G°$ as ice dries out. A remarkable exception to this pattern is TMAO, which stands out for the invariance of the denaturation curve at all V_L examined.

The thermodynamic parameters as a function of V_L are reported in Table 2 and are conveniently displayed in Figure 4. For NaCl reference the data confirm the progressive decrease of $\Delta G°$ at small V_L, about 3.5 kcal/mol between $V_L = 53\%$ and 0.53% (Figure 4, top panel), demonstrating that expansion of the solid phase can lower significantly the stability of azurin, a phenomenon we have referred to as the "ice perturbation". The trend is remarkably similar in the presence of sarcosine. The only difference relative to salt reference is a slightly larger $\Delta G°$ throughout, presumably a remnant of the osmolyte stabilization in fluid solutions. In the presence of betaine $\Delta G°$ is initially maintained large with no evidence of ice-induced instability down to $V_L = 2.7\%$. However, protection by betaine drops sharply thereafter and at $V_L = 0.53\%$ the effect is in good part lost. With TMAO the ice perturbation is totally inhibited, the protein stability being, within experimental error, practically identical all the way from the liquid solution to the driest ice. Thus, while the three methylamines have comparable effects on protein stability in liquid solutions, they exhibit a remarkably different effectiveness with regard to the ice perturbation. At one extreme, sarcosine is totally unproductive and even loses part of the stabilizing influence exerted in the liquid state. At the other, TMAO totally neutralizes the ice perturbation maintaining a constantly high protein stability in frozen and in liquid solutions. Up to now TMAO is the only compound among the osmolytes examined to exhibit full protection against the decrease in protein stability in frozen media. Betaine is intermediate, losing its efficacy only as ice dries out.

The central panel of Figure 4 points out that the decrease in protein stability as ice dries out is in all cases directly linked to the reduction in m-value. This is confirmed by the observation that the ratio $\Delta G°/m = D_{1/2}$ is largely independent of V_L (Figure 4, bottom panel). The direct correlation established between the magnitude of the m-value and the change in solvent-accessible surface area of the macromolecule on unfolding (ΔASA) (*39, 40*) suggests that the decreased stability in ice is associated to a marked reduction of ΔASA between N and D states. In other words, the interaction with ice changes the structure of either native or denatured state, or both.

Concentration Dependence of TMAO Effects in Ice. The singular performance of TMAO in countering the ice perturbation of azurin prompted an enquiry on the minimum concentration threshold required for full protection. New denaturation profiles in solution and in ice ($V_L = 53\%$, 3.43%, 1.14%, and 0.53%) were obtained after reducing the TMAO concentration to 0.6 and 0.1 M, respectively. An additional V_L value, $V_L = 1.1\%$, was introduced to better define the low V_L region of ice where the balance between the ice perturbation and osmolyte stabilization is more critical.

The estimates of $\Delta G°$ and m-value obtained from these

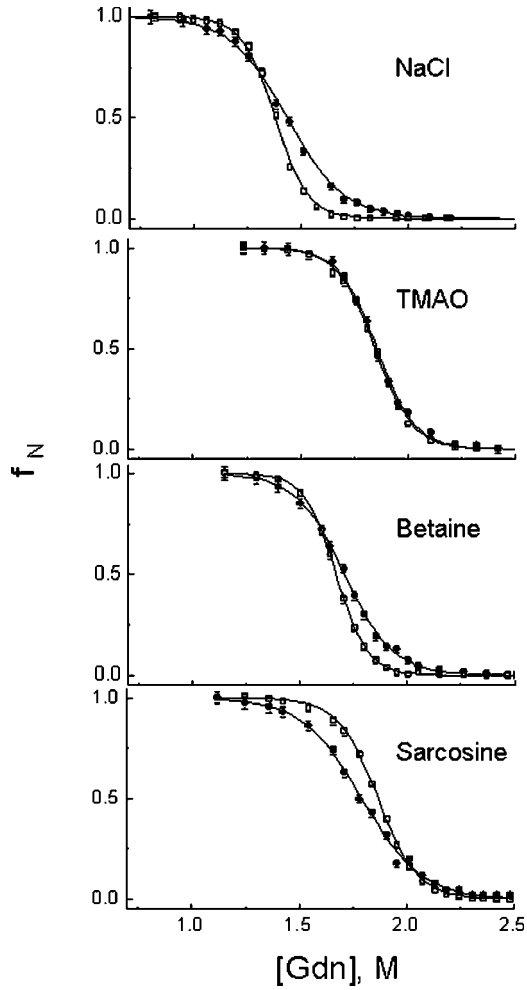

FIGURE 3: Effect of decreasing V_L from 53% (empty symbols) to 0.53% (full symbols) on equilibrium denaturation curves of C112S azurin (10 μM) in ice at –15 °C: salt reference, TMAO, betaine, and sarcosine.

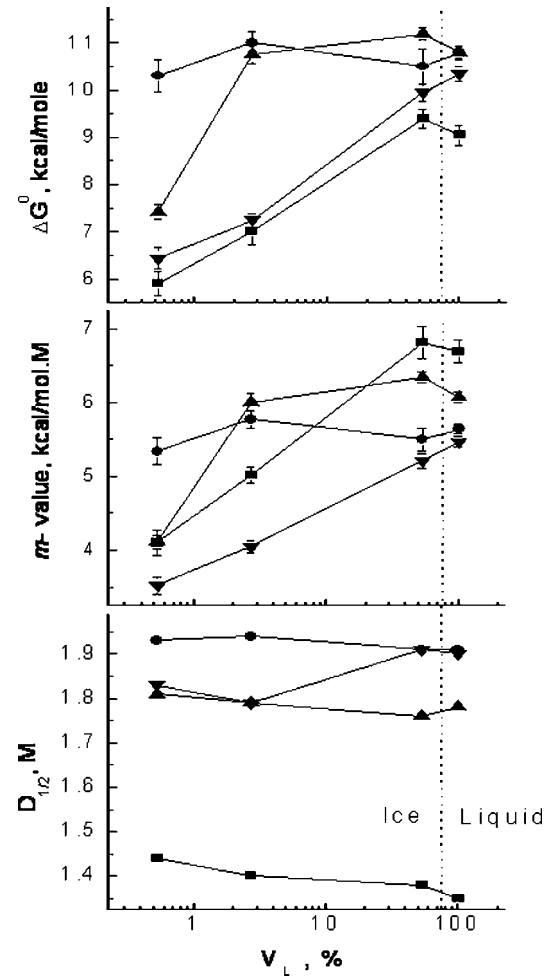

FIGURE 4: Thermodynamic parameters ($\Delta G°$, *m*-value, and $D_{1/2}$) relative to Gdn denaturation of C112S azurin at –15 °C in the liquid state and in ice of decreasing V_L: (■) salt reference; (●) TMAO; (▲) betaine; (▼) sarcosine. The data are taken from Table 2.The dotted line separates liquid from frozen samples.

profiles are reported in Figure 5. In liquid solutions the increase in $\Delta G°$ by TMAO is by and large proportional to the osmolyte concentration, as expected (*41*). In the frozen state, submolar TMAO concentrations in the liquidus provide complete protection in ice but only up to $V_L = 1.1\%$, $\Delta G°$ decreasing significantly at the smallest V_L of 0.53%. The *m*-values of Figure 5 show understandably complex trends but nevertheless indicate once again that the loss of stability in ice is correlated to the decrease in *m*-value. The implication of these results is that the addition of as little as 1.2 mM TMAO to an azurin solution in 40 mM buffer is sufficient to fully preserve the protein stability in the frozen state at −15 °C. For solutions more dilute in buffering (neutral) salts protection is incomplete unless the proportion of TMAO is increased to about 20–30% of the total solutes.

DISCUSSION

It is generally believed that the adverse effects of freezing on protein stability are owed to a combined effect of low temperature, eventually conducting to cold denaturation, and specific perturbations of the native structure induced by protein−ice interactions. For azurin $\Delta G°$ is little affected by cooling from ambient temperature to −15 °C whereas it is significantly reduced by the progressive solidification of water, a clear indication of the dominant role of protein−ice interactions in destabilizing the folded state in frozen solutions. A recent investigation aimed to dissect the contributions of ice formation, low temperature, and solute concentration toward the irreversible inhibition of catalytic activity of lactate dehydrogenase during freezing also concluded that the critical destabilizing factor is the solidification of water (*42*). The drop in $\Delta G°$ at small V_L has the characteristics of an adsorption process in which the macromolecule is partitioned between the surface of ice and the surrounding liquidus, and when bound to the interface the compact native state becomes destabilized. Indeed, as the liquid water pool shrinks, the surface area of ice per unit volume of liquidus expands rapidly, and an ever greater fraction of protein molecules will come to the interface. Protein adsorption to the solid phase was first proposed to explain the alterations of the protein tertiary structure in ice (*43*) as well as the irreversible denaturation of some proteins on freeze–thawing (*44*).

The observation that the drop of $\Delta G°$ in ice is constantly associated to the decrease in *m*-value, the ratio $\Delta G°/m = D_{1/2}$ remaining practically constant over a 200-fold variation in V_L, sheds light on the effects of protein adsorption to ice and helps to explain the different degree of protection afforded by the three methylamines. The unfolding *m*-value of different proteins has been correlated to the change in

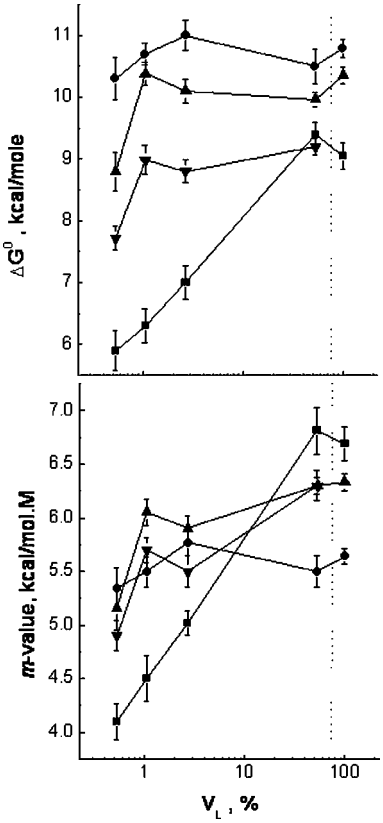

FIGURE 5: Effect of TMAO concentration on the thermodynamic parameters ($\Delta G°$, *m*-value) relative to Gdn denaturation of C112S azurin at −15 °C in the liquid state and in ice of decreasing V_L: (■) salt reference; (●) 1.2 M TMAO; (▲) 0.6 M TMAO; (▼) 0.1 M TMAO. The data are taken from Table 2. The dotted line separates liquid from frozen samples.

solvent-accessible surface area (ΔASA) between N and D states (*39, 40*). The same criterion applied to the decrease in *m*-value in ice indicates a smaller ΔASA of azurin in ice relative to the liquid state. Accordingly, adsorption of the protein to ice would result in either expansion (partial unfolding) of the N state or compaction of the D state, or both. While no information is available on the D-state structure in ice, apart from the fluorescence spectrum indicating full exposure of internal Trp-48 to the aqueous phase, there is direct spectroscopic evidence of a progressive partial unfolding of N at smaller V_L. The phosphorescence lifetime of internal Trp residues in several proteins, azurin included, reports a drastic enhancement of the structural flexibility of the macromolecule at small V_L ice, consistent with considerable loosening of the compact protein core (*43*). Likewise, ice-induced binding of ANS to proteins confirms that in frozen solutions the globular structure is generally perturbed, tending to evolve into a molten globule like state (*45, 46*). Both Trp phosphorescence and ANS binding probes report an expanded N-state that may largely account for the parallel decrease of $\Delta G°$ and *m*-value observed in the salt reference.

The addition of TMAO maintains a constant *m*-value in liquid and frozen solutions, implying that ΔASA, and presumably the compaction of the N fold, is the same in ice as in liquid solution. Such a result could be accomplished by either preventing protein adsorption to ice or by force folding native proteins at the interface. The former is a surface phenomenon that requires alterations of the ice−liquidus interface; the latter is a response to the solvophobic properties of the osmolyte responsible for the general increase in protein stability in liquid solutions. We will argue that only the surface effect hypothesis is consistent with experimental data and provides a molecular explanation for the singular effectiveness of TMAO among the osmolytes tested.

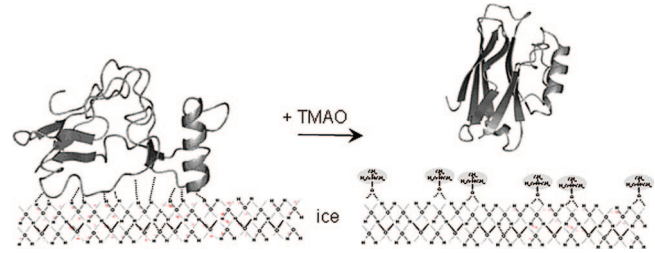

FIGURE 6: Cartoon representation of TMAO binding to ice and consequent protein desorption−refolding.

The magnitude of the solvophobic effect of an osmolyte is expected to be directly correlated to the positive free energy of transfer of the peptide backbone unit, ΔG_{tr}, from water to the aqueous osmolyte solution (*22–24, 47*). As ΔG_{tr} ranks in the order TMAO > betaine > sarcosine, this hypothesis predicts correctly that among the three methylamines TMAO be the most effective and sarcosine the least effective to counteract the ice perturbation. However, the difference in ΔG_{tr} among the three methylamines (relative to TMAO ΔG_{tr} is about 27% smaller for betaine and 44% smaller for sarcosine, respectively) (*47*) hardly accounts for the all or none protection exhibited by TMAO and sarcosine, respectively. The incongruity is even greater in the specific case of azurin as a similar increase of $\Delta(\Delta G°)$ among the three methylamines in the liquid state at −15 °C presupposes a comparable solvophobic effect in ice. Further, while the extent of solvophobic stabilization is expected to be proportional to the osmolyte concentration (*24, 41*), the effectiveness of TMAO to counter the ice perturbation remains high down to a concentration of 0.1 M where stabilization in the liquid state is negligible.

Protein adsorption to ice may be inhibited by coating the surface with a protein-repulsive molecular layer. It can also be modulated by the ice morphology, the surface area in contact with the liquidus being smallest when large ice crystals of compact shape are formed. Although we have not characterized the ice morphology, visual inspection of frozen samples reveals that in the presence of TMAO the typically whitish, fine-grain ice becomes translucent and a weaker scatterer of optical radiation, phenomena that may be tied to an increase in crystal size but also to a change in reflectivity of the ice interface.

Here we advance the hypothesis that the particular effectiveness of TMAO to counter the ice perturbation is linked to specific features of its molecular structure that, when the osmolyte is bound to ice, change the nature of the interface from attractive to repulsive with respect to polypeptides. TMAO cannot H-bond to itself but forms very strong H-bonds to water (*48*). Bound to ice it forms an ordered layer that exposes the trimethylamine moiety to the liquidus and builds up a nonpolar interface from which polypeptides tend to be excluded (Figure 6). In fact, it is the repulsive interaction between the nonpolar head of TMAO and the peptide backbone unit that is mainly responsible for the solvophobic effect of the osmolyte (*41*). In support of a

surface phenomenon is also the nonlinear concentration dependence of TMAO protection, the relatively low saturation threshold (less than 0.1 M at $V_L = 1.1\%$) being typical of monolayer coverage in a Langmuir-type chemisorption isotherm.

An ice-coating mechanism also accounts for the ineffectiveness of sarcosine to counter the ice perturbation because, in this case, specific differences in molecular structure prevent the formation of a protein-repulsive layer. Unlike TMAO, sarcosine is a classical zwitterion that can H-bond to itself and partake to ion pairing particularly in high salt media, competing interactions that lower its affinity to ice. More importantly, the molecule can H-bond to water at both carboxy and amino ends, and therefore when sarcosine is H-bonded to ice, it does not conduct to an ordered osmolyte layer of uniform composition. The new interface will expose to the liquidus charged moieties, both positive and negative, offering ample possibilities of interactions with proteins. In the case of betaine some molecular features are common to sarcosine (e.g., large dipole moment) and others to TMAO (single end H-bond), and that may explain its intermediate behavior. Betaine can H-bond to water only at the carboxy end of the molecule, and this trait will cause a preferential alignment of the osmolyte bound to the ice surface, again with the nonpolar ends facing the liquidus. However, because of the stronger repulsive electrostatic interaction between aligned dipoles the density of preferentially aligned betaine molecules on the ice surface will be kept lower, relative to TMAO. The dipole moment of betaine is about three times larger than that of TMAO (12 vs 4.2 D) (*49, 50*), and that makes the repulsive potential between neighboring osmolytes 9-fold greater.

In summary, the efficacy of TMAO to preserve the native fold of azurin in ice stands well above that of the other methylamines and polyhydric compounds examined to date. Should its action extend to proteins in general, the osmolyte could play an important and as yet unsuspected role in the cryoprotection of organisms accumulating this osmolyte. The strategy of blocking protein adsorption to the solid ice phase, if confirmed experimentally, would be alternative to that apparently operating with sugars and polyols where degradation processes are kinetically inhibited by the formation of a viscous glass-like medium (*51, 52*). In any event, TMAO protection is achieved maintaining a fluid aqueous phase and, therefore, without the need to halt biological function. As in counteracting the inhibition of enzymatic activity by urea, TMAO seems to neutralize the perturbation by making strong interactions directly with the destabilizing agent, ice or urea (*48*). On a practical side, the low concentration required for full protection could make this natural compound an attractive excipient of protein formulations used to stabilize pharmacoproteins during industrial freeze-drying processes.

REFERENCES

1. Franks, F. (1985) *Biophysics and biochemistry at low temperature*, Cambridge University Press, London.
2. Yancey, P. H., Clark, M. E., Hand, S. C., Bowlus, R. D., and Somero, G. N. (1982) Living with water stress: evolution of osmolyte systems. *Science 217*, 1214–1222.
3. Hochachka, P. W., and Somero, G. N. (2002) *Biochemical Adaptation. Mechanism and Process in Physiological Evolution*, Oxford University Press, Oxford, U.K.
4. Yancey, P. H. (2005) Organic osmolytes as compatible, metabolic and counteracting cytoprotectants in high osmolarity and other stresses. *J. Exp. Biol. 208*, 2819–2830.
5. Burg, M. B. (1995) Molecular basis of osmotic regulation. *Am. J. Physiol. 268*, F983–F996.
6. Qu, Y., Bolen, C. L., and Bolen, D. W. (1998) Osmolyte-driven contraction of a random coil protein. *Proc. Natl. Acad. Sci. U.S.A. 95*, 9268–9273.
7. Bowlus, R. D., and Somero, G. N. (1979) Solute compatibility with enzyme function and structure: rationales for the selection of osmotic agents and end-products of anaerobic metabolism in marine invertebrates. *J. Exp. Zool. 208*, 137–151.
8. Somero, G. N. (1986) Protons, osmolytes, and fitness of internal milieu for protein function. *Am. J. Physiol. 251*, R197–R213.
9. Wang, A., and Bolen, D. W. (1996) Effect of proline on lactate dehydrogenase activity: testing the generality and scope of the compatibility paradigm. *Biophys. J. 71*, 2117–2122.
10. Lin, T. Y., and Timasheff, S. N. (1994) Why do some organisms use a urea-methylamine mixture as osmolyte? Thermodynamic compensation of urea and trimethylamine N-oxide interactions with protein. *Biochemistry 33*, 12695–12701.
11. Wang, A., and Bolen, D. W. (1997) A naturally occurring protective system in urea-rich cells: mechanism of osmolyte protection of proteins against urea denaturation. *Biochemistry 36*, 9101–9108.
12. Baskakov, I., and Bolen, D. W. (1998) Time-dependent effects of trimethylamine-N-oxide/urea on lactate dehydrogenase activity: an unexplored dimension of the adaptation paradigm. *Biophys. J. 74*, 2658–2665.
13. Baskakov, I., Wang, A., and Bolen, D. W. (1998) Trimethylamine-N-oxide counteracts urea effects on rabbit muscle lactate dehydrogenase function: a test of the counteraction hypothesis. *Biophys. J. 74*, 2666–2673.
14. Arakawa, T., and Timasheff, S. N. (1985) The stabilization of proteins by osmolytes. *Biophys. J. 47*, 411–414.
15. Mello, C. C., and Barrick, D. (2003) Measuring the stability of partly folded proteins using TMAO. *Protein Sci. 12*, 1522–1529.
16. Ratnaparkhi, G. S., and Varadarajan, R. (2001) Osmolytes stabilize ribonuclease S by stabilizing its fragments S protein and S peptide to compact folding-competent states. *J. Biol. Chem. 276*, 28789–28798.
17. Yancey, P. H., and Somero, G. N. (1979) Counteraction of urea destabilization of protein structure by methylamine osmoregulatory compounds of elasmobranch fishes. *Biochem. J. 183*, 317–323.
18. Baskakov, I. V., Kumar, R., Srinivasan, G., Ji, Y. S., Bolen, D. W., and Thompson, E. B. (1999) Trimethylamine N-oxide-induced cooperative folding of an intrinsically unfolded transcription-activating fragment of human glucocorticoid receptor. *J. Biol. Chem. 274*, 10693–10696.
19. Kumar, R., Lee, J. C., Bolen, D. W., and Thompson, E. B. (2001) The conformation of the glucocorticoid receptor af1/tau1 domain induced by osmolyte binds co-regulatory proteins. *J. Biol. Chem. 276*, 18146–18152.
20. Brown, C. R., Hong-Brown, L. Q., Biwersi, J., Verkman, A. S., and Welch, W. J. (1996) Chemical chaperones correct the mutant phenotype of the delta F508 cystic fibrosis transmembrane conductance regulator protein. *Cell Stress Chaperones 1*, 117–125.
21. Raymond, J. A., and DeVries, A. L. (1998) Elevated concentrations and synthetic pathways of trimethylamine oxide and urea in some teleost fishes of McMurdo Sound, Antarctica. *Fish Physiol. Biochem. 18*, 387–398.
22. Auton, M., and Bolen, D. W. (2005) Predicting the energetics of osmolyte-induced protein folding/unfolding. *Proc. Natl. Acad. Sci. U.S.A. 102*, 15065–15068.
23. Liu, Y., and Bolen, D. W. (1995) The peptide backbone plays a dominant role in protein stabilization by naturally occurring osmolytes. *Biochemistry 34*, 12884–12891.
24. Venkatesu, P., Lee, M. J., and Lin, H. M. (2007) Thermodynamic characterization of the osmolyte effect on protein stability and the effect of GdnHCl on the protein denatured state. *J. Phys. Chem. B 111*, 9045–9056.
25. Franks, F. (2007) *Freeze-drying of pharmaceuticals and biopharmaceuticals*, RSC Publishing, Cambridge, U.K.
26. Strambini, G. B., and Gonnelli, M. (2007) Protein stability in ice. *Biophys. J. 92*, 2131–2138.
27. Nozaki, Y. (1972) The preparation of guanidine hydrochloride. *Methods Enzymol. 26*, 43–50.
28. Creighton, T. E. (1989) *Protein structure, a practical approach* (Rickwood, D., Ed.) Oxford University Press, Oxford, New York, and Tokyo.

29. Karlsson, B. G., Pascher, T., Nordling, M., Arvidsson, R. H., and Lundberg, L. G. (1989) Expression of the blue copper protein azurin from *Pseudomonas aeruginosa* in *Escherichia coli*. *FEBS Lett. 246*, 211–217.
30. Sandberg, A., Leckner, J., Shi, Y., Schwarz, F. P., and Karlsson, B. G. (2002) Effects of metal ligation and oxygen on the reversibility of the thermal denaturation of *Pseudomonas aeruginosa* azurin. *Biochemistry 41*, 1060–1069.
31. Bhatnagar, B. S., Cardon, S., Pikal, M. J., and Bogner, R. H. (2005) Reliable determination of freeze-concentration using DSC. *Thermochim. Acta 425*, 149–163.
32. Paladini, A. A., Jr., and Weber, G. (1981) Pressure-induced reversible dissociation of enolase. *Biochemistry 20*, 2587–2593.
33. Pace, C. N. (1986) Determination and analysis of urea and guanidine hydrochloride denaturation curves. *Methods Enzymol. 131*, 266–280.
34. Pace, C. N., and Shaw, K. L. (2000) Linear extrapolation method of analyzing solvent denaturation curves. *Proteins, Suppl. 4*, 1–7.
35. Santoro, M. M., and Bolen, D. W. (1988) Unfolding free energy changes determined by the linear extrapolation method. 1. Unfolding of phenylmethanesulfonyl alpha-chymotrypsin using different denaturants. *Biochemistry 27*, 8063–8068.
36. Sandberg, A., Leckner, J., and Karlsson, B. G. (2004) Apo-azurin folds via an intermediate that resembles the molten-globule. *Protein Sci. 13*, 2628–2638.
37. Singh, R., Haque, I., and Ahmad, F. (2005) Counteracting osmolyte trimethylamine N-oxide destabilizes proteins at pH below its pKa. Measurements of thermodynamic parameters of proteins in the presence and absence of trimethylamine N-oxide. *J. Biol. Chem. 280*, 11035–11042.
38. Holthauzen, L. M., and Bolen, D. W. (2007) Mixed osmolytes: the degree to which one osmolyte affects the protein stabilizing ability of another. *Protein Sci. 16*, 293–298.
39. Courtenay, E. S., Capp, M. W., Saecker, R. M., and Record, M. T., Jr (2000) Thermodynamic analysis of interactions between denaturants and protein surface exposed on unfolding: interpretation of urea and guanidinium chloride m-values and their correlation with changes in accessible surface area (ASA) using preferential interaction coefficients and the local-bulk domain model. *Proteins, Suppl. 4*, 72–85.
40. Myers, J. K., Pace, C. N., and Scholtz, J. M. (1995) Denaturant m values and heat capacity changes: relation to changes in accessible surface areas of protein unfolding. *Protein Sci. 4*, 2138–2148.
41. Street, T. O., Bolen, D. W., and Rose, G. D. (2006) A molecular mechanism for osmolyte-induced protein stability. *Proc. Natl. Acad. Sci. U.S.A. 103*, 13997–14002.
42. Bhatnagar, B. S., Pikal, M. J., and Bogner, R. H. (2007) Study of the individual contributions of ice formation and freeze-concentration on isothermal stability of lactate dehydrogenase during freezing. *J. Pharm. Sci. 12*, 505–523.
43. Strambini, G. B., and Gabellieri, E. (1996) Proteins in frozen solutions: evidence of ice-induced partial unfolding. *Biophys. J. 70*, 971–976.
44. Chang, B. S., Kendrick, B. S., and Carpenter, J. F. (1996) Surface-induced denaturation of proteins during freezing and its inhibition by surfactants. *J. Pharm. Sci. 85*, 1325–1330.
45. Gabellieri, E., and Strambini, G. B. (2003) Perturbation of protein tertiary structure in frozen solutions revealed by 1-anilino-8-naphthalene sulfonate fluorescence. *Biophys. J. 85*, 3214–3220.
46. Gabellieri, E., and Strambini, G. B. (2006) ANS Fluorescence Detects Widespread Perturbations of Protein Tertiary Structure in Ice. *Biophys. J. 90*, 3239–3245.
47. Auton, M., and Bolen, D. W. (2004) Additive transfer free energies of the peptide backbone unit that are independent of the model compound and the choice of concentration scale. *Biochemistry 43*, 1329–1342.
48. Paul, S., and Patey, G. N. (2007) Structure and interaction in aqueous urea-trimethylamine-N-oxide solutions. *J. Am. Chem. Soc. 129*, 4476–4482.
49. Price, W. D., Jockusch, R. A., and Williams, E. R. (1998) Binding energies of protonated betaine complexes: a probe of zwitterion structure in the gas phase. *J. Am. Chem. Soc. 120*, 3474–3484.
50. Shikata, T., and Itatani, S. (2002) Dielectric relaxation of aqueous trimethylamineoxide solutions. *J. Solution Chem. 31*, 823–844.
51. Chang, L. L., Shepherd, D., Sun, J., Ouellette, D., Grant, K. L., Tang, X. C., and Pikal, M. J. (2005) Mechanism of protein stabilization by sugars during freeze-drying and storage: native structure preservation, specific interaction, and/or immobilization in a glassy matrix? *J. Pharm. Sci. 94*, 1427–1444.
52. Tang, X. C., and Pikal, M. J. (2005) Measurement of the kinetics of protein unfolding in viscous systems and implications for protein stability in freeze-drying. *Pharm. Res. 22*, 1176–1185.

BI702473G